Weldability of a Ni-Cu-Cb Line-Pipe Steel

A new steel with improved strength and fracture toughness is shown to have good weldability characteristics that will meet the welding requirements of pipeline steels for low-temperature service

BY J. GORDINE

ABSTRACT. The weldability of an experimental Ni-Cu-Cb line-pipe steel designed for low-temperature service was compared to that of a conventional C-Mn X65 line-pipe steel. Using conventional weldability tests it was shown that the weldability of the Ni-Cu-Cb steel was superior to the C-Mn steel. Heat-affected zone (HAZ) simulation experiments using the Gleeble also showed that the HAZ toughness properties of the Ni-Cu-Cb steel were superior to the C-Mn steel.

It was concluded that the weldability characteristics of the Ni-Cu-Cb steel were good and would meet the welding requirements of pipeline steels for low-temperature service applications.

Introduction

The construction of gas or oil transmission pipelines in northern climates has set very high demands upon the materials to be used in these pipelines. Considerable progress has been made in recent years in improving existing steels and developing new steels for these northern pipeline applications. Major emphasis has been on improving the strength and fracture toughness characteristics of these steels. Considerably less attention has been given to examining the weldability of these steels. However, a prime requirement of any material used for northern pipelines is that it should possess good weldability.

The purpose of the work described in this paper was to compare the weldability of one of these new pipeline steels, a Ni-Cu-Cb steel, with that of a conventional line-pipe steel of the type now being used for conventional applications.

Materials

The Ni-Cu-Cb steel was received as a 6 ft (1.8 m) section of an experimental length of pipe, with a 30 in. (762 mm) O.D. by ⅜ in. (9.6 mm) wall thickness. The conventional line-pipe steel was a 38 ft (11.6 m) length of commercial quality pipe with a 36 in. (914 mm) O.D. and 0.518 in. (13.2 mm) wall thickness. This particular pipe was manufactured to API 5LX-1971, Grade 65.

The chemical compositions of the two line-pipe steels are shown in Table 1. Their compositions are considerably different. The conventional line-pipe steel, referred to as line-pipe F, is basically a C-Mn steel with moderate Cb and V additions combined with some controlled rolling to bring up its strength level. The microstructure of this steel is a heavily banded ferrite-pearlite structure as shown in Fig. 1A.

The Ni-Cu-Cb steel, referred to as line-pipe A, has much lower C and Mn contents and achieves its strength by alloying additions of Ni, Cu, Cb, Cr and Mo. This is an age-hardening steel, the primary precipitation-hardening element being Cu. The Ni and Cb contents impart good fracture toughness as well as additional strengthening. The function of the Cr and Mo additions, apart from their direct contribution to strength, is to control the precipitation kinetics of the Cu such that the optimum combination of strength and toughness can be achieved.

The microstructure of line-pipe A is shown in Fig. 1B. It differs from that of line-pipe F in that its grain size is finer and it has a much lower volume fraction of pearlite; also its microstructure is not banded.

The tensile properties for the two steels, taken transverse to the pipe axis (i.e., transverse to the original rolling direction), are listed in Table 2. The data for line-pipe A are for pipe supplied in the rolled-and-aged condition. The aging treatment used, after fabrication of the pipe, was 704 C (1300 F) for 30 min.

The toughness properties for the two steels as measured by the Charpy impact test are shown in Fig. 2. The data shown are for ⅔ size specimens taken transverse to the original rolling direction of the pipe. The superiority

J. GORDINE is a Research Scientist with the Welding Section, Physical Metallurgy Research Laboratories, CANMET, Department of Energy, Mines and Resources, Ottawa, Canada.

Table 1—Chemical Compositions of Two Line-Pipe Steels, %

	Steel A	Steel F
C	0.04	0.161
Mn	0.44	1.34
P	0.010	0.006
S	0.015	0.009
Si	0.28	0.33
Ni	0.89	–
Cu	1.16	–
Cb	0.04	0.031
Cr	0.68	–
Mo	0.21	–
V	–	0.046

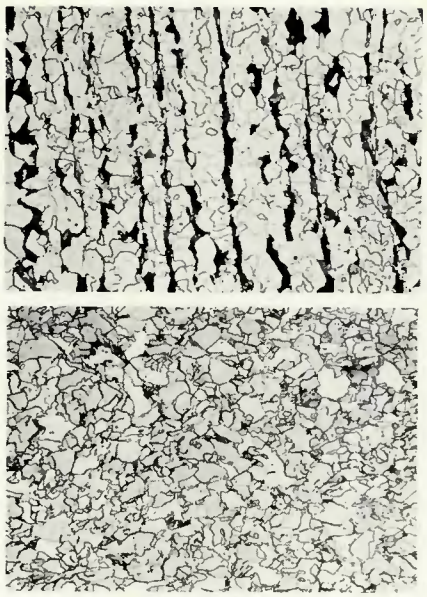

Fig. 1—Microstructures of two line-pipe steels: A (top)—line-pipe F; B (bottom)—line-pipe A. ×400 (reduced 46% on reproduction)

of line-pipe A steel in respect to low-temperature toughness is very evident. Further improvement in toughness may be achieved in this steel by using a quenching or normalizing treatment prior to aging. For the purpose of this study, only the rolled-and-aged condition was considered.

Experimental Procedures

Metallography

Samples for metallographic examination were prepared by grinding down to 600-grit paper and polishing through to ¼ μ diamond paste. Etching was done in 2% nital.

Hardness Testing

Hardness tests were carried out using a Vickers hardness testing machine with a 10 kg load. Microhardness tests were made with a Wilson hardness tester using a 500 g load.

Tensile Testing

Tensile tests were made using strap-type tensile specimens of full wall thickness with 2 in. (50 mm) gauge length, according to the requirements of API 5LX-1971. All tests were made at room temperature.

Charpy V-Notch Testing

Charpy V-notch ⅔ size specimens were used in most tests. Tests were made over a range of temperatures of sufficient extent to establish the full transition curve. Five specimens were tested per temperature for weld specimens and three per temperature for HAZ specimens. Accurate placement of the notch was ensured by etching and scribing the metal in the vicinity of the notch prior to notching.

Welding Procedures

Welding procedures used were based on conventional field-welding procedures that are currently used for the welding of the circumferential girth joints of high-strength line-pipe.[1]

Controlled Thermal Severity (CTS) Testing

The susceptibility to HAZ cold cracking was assessed by the CTS test. The actual test assembly used is shown in Fig. 3. The anchor welds were deposited with E7018 electrodes. The test fillet welds were deposited with 5/32 in. (4 mm) E7010 electrodes using a constant energy input of 20,000 Joules/in. (780 Joules/mm). Sufficient time was allowed between deposition of the two test welds to allow the specimen to regain the test temperature.

After welding, the specimen was allowed to stand at the test temperature for 48 h. Each test weld was then sectioned at three equally spaced locations and examined for cracking by the wet fluorescent magnetic particle method. Selected sections were also examined metallographically, and hardness traverses were made. The CTS tests were conducted in a refrigerated room that enabled the test temperature to be varied from room temperature down to −36 C (−33 F).

Bead-on-Plate Tests

Bead-on-plate tests were conducted on 2 × 3 in. (50 × 76 mm) specimens of full wall thickness cut from the pipe. The 1.25 in. (32 mm) test weld was deposited with 1/8 in. (3 mm) diameter E7010 electrodes at a constant energy input of 15,000 Joules/in. (590 Joules/mm).

Tests were made in a refrigerated room with the specimens suspended in a bath containing ethylene glycol such that the liquid level was maintained 0.25 in. (6 mm) below the top

Table 2—Tensile Properties of Two Line-Pipe Steels

	Steel A	Steel F
Yield stress, ksi (MPa)	84.0 (580)	67.2 (462)
Ultimate tensile strength, ksi (MPa)	87.0 (600)	91.8 (634)
Elongation in 2 in. (50 mm), %	29	32

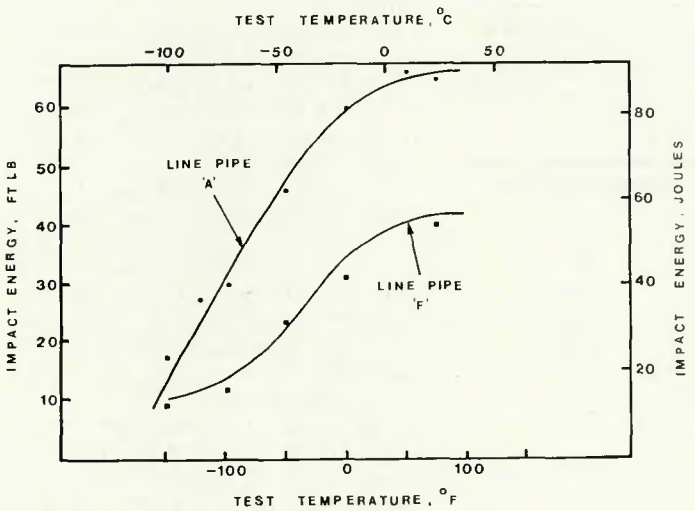

Fig. 2—Charpy V-notch impact properties of two line-pipe steels: 2/3 size specimens taken transverse to rolling direction

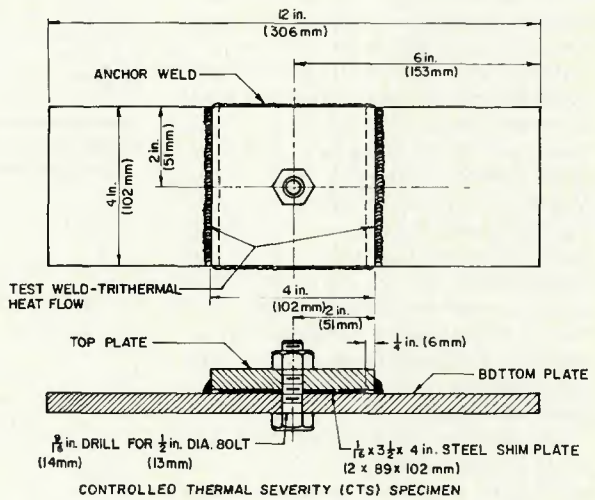

Fig. 3—CTS test weldability specimen

Table 3—Welding Parameters for Manual Welding of Test Coupons[a]

	Root pass	Filling pass
Volts, V	26	24
Current, A	145	150
Travel speed, ipm (mm/s)	12 (5)	7 (3)
Energy input, J/in. (J/mm)	19,000 (750)	27,000 (1,060)

[a]Electrode: designation—Lincoln Shield-Arc HYP, classification—AWS 7010, diameter—5/32 in. (4 mm). DCRP; welding position—vertically downward; joint preparation—60 deg included angle with 1/16 in. (1.5 mm) root face.

surface of the specimen. After deposition of the test weld, the specimens were held 24 h at the test temperature prior to sectioning longitudinally and examining for cracking.

Five specimens were tested per temperature. The test temperatures varied from room temperature down to −36 C (−33 F). The total crack length in the HAZ was measured and recorded as a percentage of the total weld length.

HAZ Simulation Tests

HAZ microstructures were simulated in ⅔ size Charpy specimens using the R.P.I. Gleeble apparatus. The thermal cycles imposed on the specimens were the most rapid in terms of cooling that could be achieved in the Gleeble; they closely approximated the most severe thermal cycles likely to be encountered during manual field welding.[2]

Four peak temperatures were used; they were 1300, 1100, 900 and 700 C (2370, 2010, 1650 and 1290 F).

Experimental Results

Work Program

The work program was designed to evaluate three aspects of weldability:

1. To compare the field welding behavior of the two steels by conducting laboratory welding tests using conventional field welding procedures.
2. To compare the relative susceptibilities of the two steels to HAZ cracking by conducting suitable weldability tests.
3. To compare the HAZ toughness of the two steels.

Comparison of Field Welding Behavior

The conventional method of welding the circumferential girth weld in pipeline construction is by the manual shielded metal arc process. Although this may not be a suitable technique for some northern pipeline applications, it does impose very severe demands on material properties. It was, therefore, a convenient means by which to compare the welding characteristics of the two steels.

Test coupons of the two steels were welded together in the laboratory using the welding conditions listed in Table 3. The welding electrodes used were E7010 and are manufactured specifically for the welding of high-strength line-pipe steels.

Welding was done at room temperature, and some tests were also conducted in the cold room at temperatures as low as −20 C (−4 F). No preheating was used in any of the tests. After welding, the test welds were radiographically examined using X-rays.

The results of this work indicated that the welding characteristics of both steels were excellent. No difficulties were encountered in producing welds to meet the field welding standards of acceptability defined by API 1104 or CSA Z184. Where defects were observed, they could be traced to improper welding procedures. No HAZ cracking was encountered in any welds despite the low ambient temperatures used for some tests and the high hydrogen potential of the cellulosic electrodes.

Sections were taken through the completed welds, and hardness traverses were made across the weld and HAZ. The results are shown in Figs. 4 and 5. The hardnesses for line-pipe A were slightly higher in both the weld and HAZ.

Toughness properties for the welds were also determined, and these are shown in Fig. 6. The data for line-pipe F were for full-size Charpy specimens; this will explain the higher values obtained.

Comparison of Weldability

The two tests used for comparing weldability—the CTS and the bead-on-plate—are both designed to evaluate the susceptibility of a material to HAZ cracking due to hydrogen. This is a serious potential problem in the welding of pipeline steels, particularly when using the conventional manual welding process.

The results of the CTS tests conducted on the two steels are summarized in Table 4. The results clearly demonstrate the superior resistance of

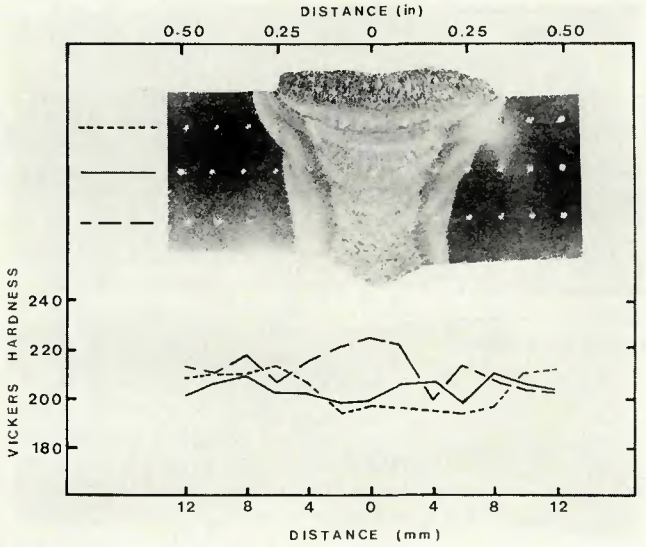

Fig. 4—Macrosection and hardness survey of manual weld in line-pipe A

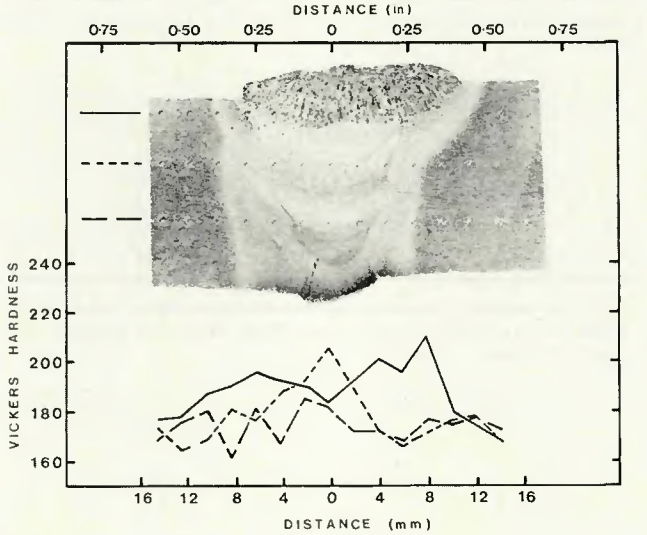

Fig. 5—Macrosection and hardness survey of manual weld in line-pipe F

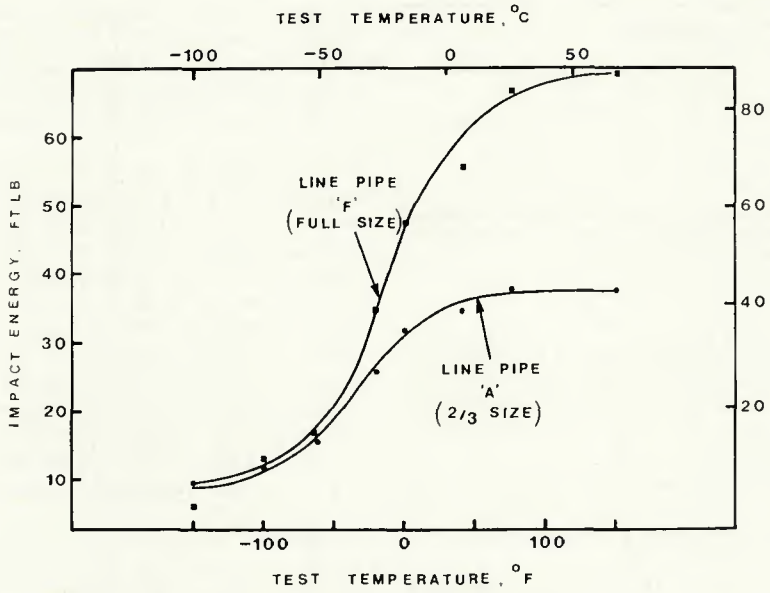

Fig. 6—Impact transition curves for manual 7010 welds in two line-pipe steels

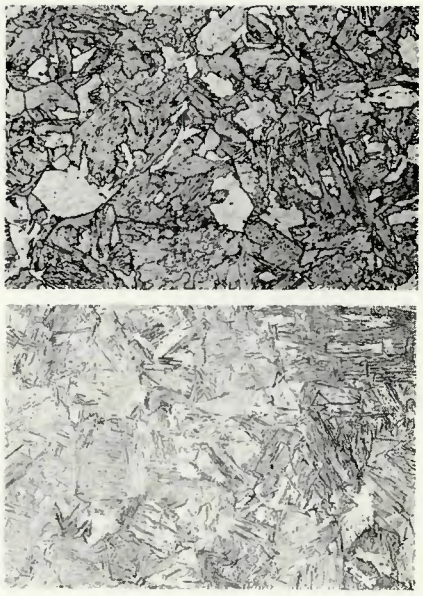

Fig. 7—Microstructures of coarse-grained regions of HAZ of two line-pipe steels: A (top)—line-pipe A; B (bottom)—line-pipe F. ×400 (reduced 46% on reproduction)

line-pipe A to HAZ cracking. No cracking could be induced in the HAZ even at the lowest test temperature. Line-pipe F, however, exhibited extensive HAZ cracking, under identical welding conditions, at test temperatures of +4 C (+39 F).

Micro-hardness traverses were made across selected specimens, and the results showed that much higher hardness levels were produced in the HAZ of line-pipe F than in line-pipe A. A maximum hardness of 460 Vickers hardness number (VHN) was recorded in line-pipe F compared with a maximum of 318 in line-pipe A. In both cases, the maximum hardness occurred in the coarse-grained region of the HAZ close to the fusion boundary. The cracking observed in line-pipe F was also concentrated in this region. The microstructures of the coarse-grained regions of the two steels are shown in Fig. 7. The more acicular martensitic appearance of this zone in line-pipe F is very evident.

Similar results, confirming the superior resistance of line-pipe A to HAZ cracking, were obtained in the bead-on-plate tests. These results are summarized in Table 5. Line-pipe F showed HAZ cracking at room temperature, with the amount of cracking generally increasing as the test temperature was lowered. Under identical welding conditions, no HAZ cracking was observed in line-pipe A at any test temperature. Hardness measurements made across the HAZ also confirmed much higher HAZ hardness in line-pipe F.

Comparison of HAZ Toughness

A comparative measure of the toughness properties in the HAZ of the two steels was achieved using the Gleeble. The maintenance of adequate toughness in the HAZ will be one of the considerations in the ultimate selection of materials for northern pipelines. There is no doubt that specifications for Arctic pipelines will include toughness requirements on the weld and HAZ for both the girth welds and the seam welds. The measurement of toughness in the HAZ is, however, difficult due to the narrow width of the HAZ and also the lack of uniformity of properties across its width.

One solution to this problem is to use the Gleeble apparatus to reproduce selected regions of the HAZ in bar-size samples suitable for the determination of toughness. Specimens were heated and cooled through the selected thermal cycle in the Gleeble and then tested in impact loading at different test temperatures to determine the transition curve. The results for the two steels are shown in Figs. 8 and 9.

The results for line-pipe F, shown in Fig. 8, clearly indicate that the toughness across the entire width of the HAZ is inferior to the base metal notch toughness. The worst properties in terms of shelf energy and transition temperature were obtained for the 700 C (1290 F) peak temperature condition. The 1300 C (2370 F) and 900 C (1650 F) peak temperature conditions also produced a significant loss in impact properties.

Line-pipe A showed reduced impact toughness only for the 1300 C (2370 F) peak-temperature condition as shown

Table 4—Effect of Test Temperature on HAZ Cracking in CTS Tests for Two Line-Pipe Steels

Test temperature		Extent of cracking	
°C	°F	Line-pipe A	Line-pipe F
21	70	None	None
4	39	None	Extensive
−16	3	None	Extensive
−27	−17	None	Extensive
−36	−33	None	Extensive

Table 5—HAZ Cracking in Bead-on-Plate Tests as a Function of Test Temperature for Two Line-Pipe Steels

Test temperature		Percent of cracking in HAZ	
°C	°F	Line-pipe A	Line-pipe F
23	74	0	11
4	39	0	22
−16	3	0	31
−27	−17	0	28
−40	−40	0	34

in Fig. 9. The 1100 C (2010 F) and 700 C (1290 F) peak-temperature thermal cycles caused little change in impact properties other than a slight lowering of the shelf energy. The 900 C (1650 F) peak temperature actually improved the impact properties of the steel.

A comparison of the two steels in terms of their 15 ft-lb (20 J) transition temperatures is shown in Table 6. These results illustrate the overall superiority of line-pipe A with regard to HAZ toughness. Only the 1300 C (2370 F) peak temperature caused a significant raising of the 15 ft-lb (20 J) transition temperature relative to the as-received material. The remaining peak-temperature conditions actually caused a lowering of the 15 ft-lb (20 J) transition temperature.

Line-pipe F showed an increase in transition temperature for all peak-temperature conditions except for the 1100 C (2010 F) condition. The 700 C (1290 F) peak temperature had the greatest influence, increasing the 15 ft-lb (20 J) transition temperature from −51 C (−60 F), for the as-received condition, to 99 C (210 F).

Specimens corresponding to each peak-temperature condition were examined metallographically in an attempt to correlate microstructures with the observed toughness properties. These results are shown in Figs. 10 and 11.

The microstructures of the C-Mn steel (Fig. 10) could not be correlated exactly with the observed toughness properties (Fig. 8). The 700 C (1290 F) peak-temperature thermal cycle which caused the most severe loss of impact values, caused little apparent change in microstructure. The 900 C (1650 F) peak-temperature thermal cycle resulted in a fine-grained ferrite-pearlite microstructure; surprisingly, however, this did not improve the toughness properties. The 1100 C (2010 F) peak-temperature thermal cycle produced a partly martensitic microstructure, but the toughness properties were equivalent to those of the base metal.

Only the 1300 C (2370 F) peak-temperature thermal cycle produced a microstructure change that could be correlated easily to the observed toughness. In this case, the microstructure developed was martensitic with a large, prior austenite grain size. This type of structure would not be expected to exhibit good toughness.

For line-pipe A, the microstructures could be correlated more closely with the observed changes in toughness. The 900 C (1650 F) and 1100 C (2010 F) peak-temperature thermal cycles produced some refinement of grain size, thus explaining the improvement in impact properties. The 1300 C (2370 F) peak-temperature thermal cycle produced a coarse-grained microstructure similar to that observed in line-pipe F; not surprisingly, this structure showed poor toughness.

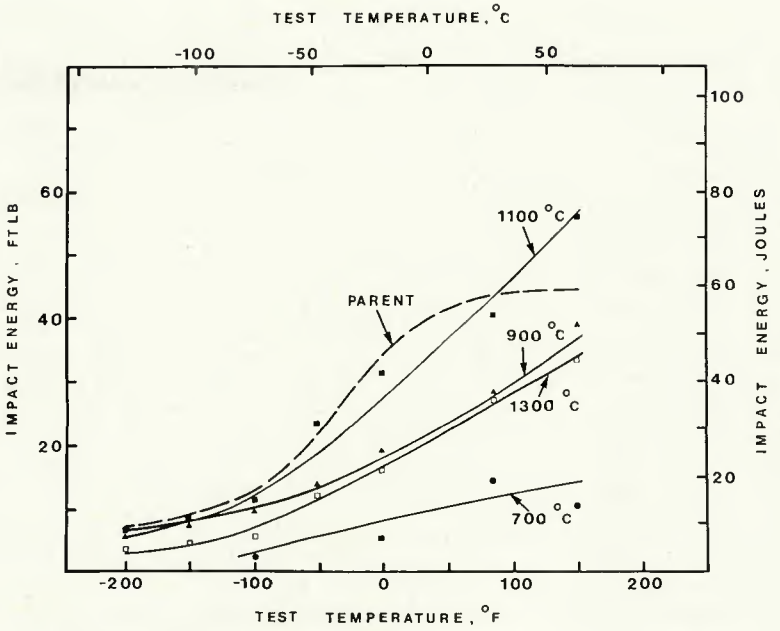

Fig. 8—Charpy V-notch impact properties of Gleeble-simulated HAZ's in line-pipe F (2/3 size specimens)

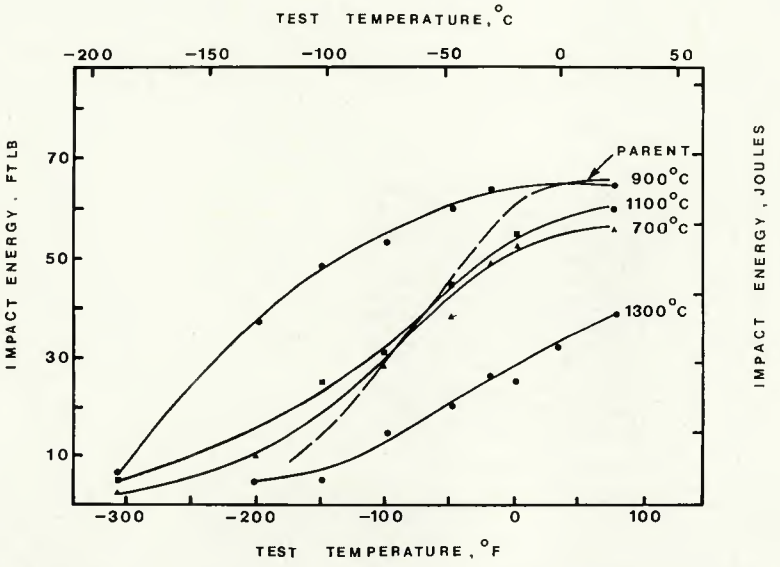

Fig. 9—Charpy V-notch impact properties of Gleeble-simulated HAZ's in line-pipe A (2/3 size specimens)

Discussion

The comparison of the welding characteristics of the two line-pipe steels has established that the weldability of the experimental line-pipe steel A is superior to that of conventional line-pipe steel F. In the weldability tests conducted, line-pipe A demonstrated a much higher

Table 6—Comparison of 15 ft-lb Transition Temperature of HAZ of Two Line-Pipe Steels

Thermal cycle peak temperature	15 ft-lb (20 J) transition temperature	
	Line-pipe A	Line-pipe F
As-received	−106 C (−160 F)	−51 C (−60 F)
700 C (1292 F)	−109 C (−165 F)	99 C (210 F)
900 C (1650 F)	−171 C (−275 F)	−38 C (−36 F)
1100 C (2012 F)	−131 C (−205 F)	−57 C (−70 F)
1300 C (2372 F)	− 62 C (−80 F)	−30 C (−22 F)

resistance to HAZ cracking than line-pipe F. This is an important characteristic that will be demanded of line-pipe steels for northern pipelines.

The greater wall thicknesses generally specified for these pipelines, combined with the low ambient temperatures, will tend to produce more rapid HAZ cooling rates. These rapid cooling rates are likely to produce martensitic microstructures in the HAZ that are very susceptible to hydrogen-induced cracking.

Line-pipe A, despite the rapid cooling rates imposed by the CT5 and bead-on-plate tests, did not develop hardened martensitic microstructures in the HAZ as did line-pipe F and hence did not show the same propensity to cracking. This is a somewhat surprising result if the carbon equivalent (CE) values for the two steels are calculated and compared. Using the most generally accepted formula,

$$CE = C + \frac{Mn}{6} + \frac{Cr + Mo + V}{5} + \frac{Ni + Cu}{15}$$

the Ni-Cu-Cb steel would have a CE of 0.42, and the C-Mn steel 0.39. The higher CE value for line-pipe F would imply a higher susceptibility to HAZ cracking, which is a direct contradiction of the observed results.

These results indicate that, at least for this particular composition, the conventional CE formula is not completely satisfactory. Sawhill[3] has reached similar conclusions and has suggested the CE relationship proposed by Ito and Bessyo[4] may be more appropriate for the low-carbon steels. Ito and Bessyo define a cracking parameter (P_c) rather than the conventional carbon equivalent factor. The formula they derived is as follows:

$$P_c = C + \frac{Si}{30} + \frac{Mn}{20} + \frac{Cu}{20} + \frac{Ni}{60} + \frac{Cr}{20} + \frac{Mo}{15} + \frac{V}{10} + 5B + \frac{t}{600} + \frac{H}{60}$$

where t = plate thickness in mm, and H is the amount of diffusible hydrogen in weld metal in cc/100 g.

Using this formula and assuming a diffusible hydrogen content of 5 cc/100 g, the P_c values for line-pipe A would be 0.28, and line-pipe F 0.33. Although this places the two steels in the correct order in regard to cracking susceptibility, the absolute values of P_c are not very meaningful. It must also be appreciated that the composition range of line-pipe A is outside those ranges to which the Ito-Bessyo relationship is strictly valid. It is clear that further research is necessary in this area to produce a CE or P_c formula that can be used for steels in this range of composition.

The HAZ toughness for the two steels, as predicted by the Gleeble results, indicated that the overall HAZ toughness of line-pipe A was superior to that of line-pipe F. In fact, much of the HAZ in line-pipe A has a finer grain size and better toughness than the base metal. Only the coarse-grained region of the HAZ, immediately adjacent to the fusion zone of the weld, exhibited reduced toughness. Line-pipe F, on the other hand, showed reduced toughness across the entire width of the HAZ, with particularly severe loss of toughness in the outer extremities of the HAZ that were exposed to a weld thermal cycle having a peak temperature of 700 C (1290 F). The latter phenomenon is not readily explainable since no gross microstructural changes were associated with this loss of toughness.

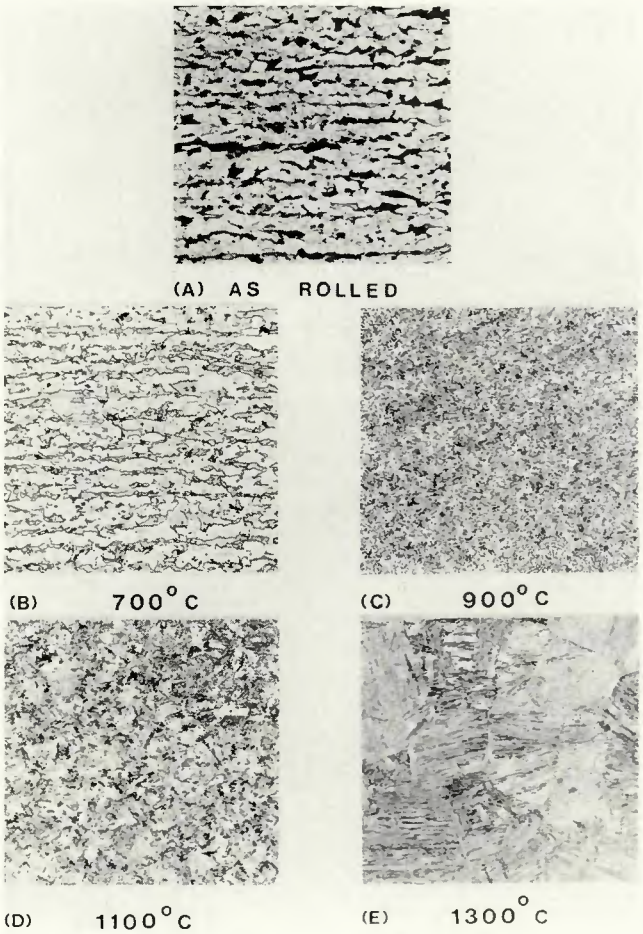

Fig. 10—Simulated HAZ microstructures in line-pipe F. ×250 (reduced 34% on reproduction)

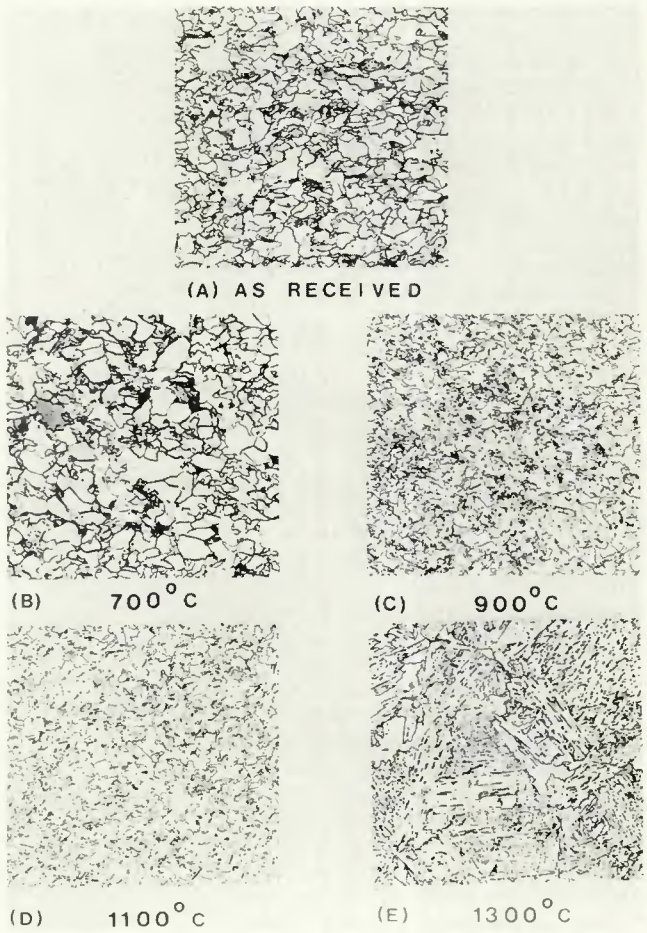

Fig. 11—Simulated HAZ microstructures of line-pipe A. ×400 (reduced 34% on reproduction)

The significance of the bands of low-toughness material within the HAZ is not clear. From a general viewpoint, it must cause an overall lowering of the ductile fracture resistance of the HAZ, which for Arctic pipeline applications is not desirable. Certainly, the extensive loss of toughness across the entire width of the HAZ observed in line-pipe F would not be acceptable for most northern applications.

In line-pipe A, where the loss of toughness is confined to the coarse-grained region of the HAZ, the properties would probably satisfy most northern requirements. It should, however, be specified that the width of this low-toughness zone be kept to a minimum by using low-energy inputs for welding.

In conventional field welding, the energy inputs used are low. Therefore, the width of the HAZ is kept to a minimum. In the submerged arc seam weld, however, energy inputs used are much higher, and here there would, therefore, be more difficulty in maintaining toughness in the HAZ. Also, since it is a two-pass welding operation, advantage cannot be taken of the refinement of the HAZ that occurs in a multipass process.

Conclusion

The primary objective of this work was to compare the welding characteristics of the experimental line-pipe steel A with those of a conventional line-pipe steel F for the purpose of evaluating its potential as an Arctic-grade line-pipe steel. The results obtained have demonstrated that, in terms of weldability, line-pipe steel A is superior to line-pipe steel F and that this level of weldability should be adequate for most line-pipe applications.

Line-pipe A is a Ni-Cu-Cb steel that could be welded by conventional processes without problems and with little loss in toughness in the HAZ. It also exhibited a very good resistance to hydrogen induced HAZ cracking. With these good weldability characteristics and its reported excellent low-temperature mechanical properties, the future of the Ni-Cu-Cb steel as an Arctic-Grade line-pipe steel is promising.

The one barrier that may limit the widespread application of Ni-Cu-Cb steel is economical. Compared to other high-strength micro-alloy steels now available, the mix costs for the Ni-Cu-Cb steel are very high, and this may limit its usage to certain critical applications or for fittings applications.

Acknowledgments

Thanks are expressed to Dr. R. J. Cooke for his significant contribution to this work. Appreciation is also expressed to Messrs. M. Letts and L. Joy who carried out the experimental work. Finally, thanks are expressed to Dr. K. Winterton for his interest in the work and his suggested modifications to the manuscript.

References

1. Looney, R. L., "Pipeline Welding—Meeting Today's Quality Requirements," Lincoln Electric Technical Bulletin M.642, January 1970.

2. Cooke, R. J., "An Evaluation of the Thermal Cycles Imposed on the HAZ during Manual Pipe Welding," Physical Metallurgy Research Laboratories Internal Report PM-R-74-21, CANMET, Department of Energy, Mines and Resources, Ottawa, Canada.

3. Sawhill, J. M., "Implant Tests of a Mn-Mo-Cb Steel and a Conventional X65 Steel," Climax Molybdenum Report, L-176-11, June 21, 1973, Ann Arbor, Michigan.

4. Ito, Y., and Bessyo, K., International Institute of Welding Document No. IX-576-68.